

Application of Image Cross-Correlation to the Measurement of Glacier Velocity Using Satellite Image Data

Theodore A. Scambos

Hughes STX Corporation, Lanham, Maryland

Melanie J. Dutkiewicz and Jeremy C. Wilson

MacDonald Dettwiler, Richmond, British Columbia, Canada

Robert A. Bindshadler

NASA Goddard Space Flight Center, Greenbelt, Maryland

Image-to-image cross-correlation software is applied to pairs of digital satellite images to map the velocity field of moving ice. This technique uses small-scale glacial surface features, such as crevasse scars and snow dunes, as markers on the surface of the moving ice. Displacements of the surface features are mapped by selecting small image areas centered on distinct features, or by dividing a large area of densely featured glacial surface into a grid of areas, and searching a subsequent image for matching areas using a cross-correlation algorithm. Interpolation of the peak correlation values allows the displacements to be measured to subpixel accuracy, resulting in very precise velocity measurements. Cross-correlation is also applied to provide image coregistration in areas devoid of bedrock exposures. In such areas, subtle large-scale topographic undulations in the

ice surface, related to underlying bedrock structure, may be correlated by using large image areas and low-pass filtered images. Both types of applications are demonstrated, using Ice Stream D and Ice Stream E in West Antarctica as test areas. A high-resolution map of the velocity field of the central portion of Ice Stream E, generated by the displacement-measuring technique, is presented. The use of cross-correlation software is a significant improvement over previous manually-based photogrammetric methods for velocity measurement, and is far more cost-effective than in situ methods in remote polar areas.

INTRODUCTION

The polar ice caps and glaciated regions form an important component of the global environment. They are critical to current climate and sea level. However, simple parameters of the dynamics of these frozen areas, such as flux and mass balance, remain very poorly known. This is due in large part

Address correspondence to Theodore A. Scambos, Code 971, Oceans and Ice Branch, NASA Goddard Space Flight Center, Greenbelt, MD 20771

Received 20 September 1991, revised 15 March 1992

to the vastness and remoteness of large portions of the cryosphere. Satellite-based remote sensing can provide quick, accurate, and relatively inexpensive information about cryosphere dynamics, if algorithms for extracting the pertinent measurements from remotely sensed data can be developed. The present study details one such algorithm, which yields velocity field determinations of moving ice, and, additionally, provides an accurate method of coregistering images in remote polar regions lacking fixed control points.

Previous studies have demonstrated the usefulness of sequential satellite imagery for glacier velocity measurements (Lucchitta and Ferguson, 1986, MacDonald et al, 1989, Lucchitta et al, 1989, Doake and Vaughan, 1991). To date, visually based photogrammetric techniques have been used, consisting of coregistering two images using bedrock outcrops, selecting surface features on the ice, visually finding their location on the subsequent image, and manually or mechanically measuring their displacement. Small, sharp surface features are required for high precision when visual techniques are used. Precisions are limited by the pixel size of the image data, since the location of any extended feature in the image is referenced to a single pixel location somewhere on the feature.

A second limitation of previous methods is the requirement that exposed bedrock be present somewhere within the imaged area for accurate coregistration of the two images. This is more

restricting than it may seem at first, large areas of the Greenland and Antarctic ice sheets, including outlet areas, are completely ice-covered. These regions can have complex ice dynamics (e.g., Stephenson and Bindshadler, 1990), and thus are important to studies of ice flux and mass balance.

The method presented here offers an improved approach to the remote measurement of ice motion. Because features are represented by small rectangular image areas (hereafter called "chips") rather than single pixels, displacements may be interpolated to subpixel accuracy. Diffuse, extended features yield precisions similar to those for sharp features. In areas without bedrock outcrops, a separate type of application of the algorithm can accurately coregister images prior to velocity measurement. Generation of a detailed map of the velocity field, with a very high density of velocity measurements, is much easier with the presented technique than with the earlier methods. Any digital image data of moderate to high resolution can be used (e.g., Landsat TM, Landsat MSS, SPOT, or digital aerial photography). The results of an initial application of the image-to-image cross-correlation technique have been previously discussed (Bindshadler and Scambos, 1991). This paper expands the discussion of the method used in that study, and demonstrates its potential by generating a high-resolution velocity field map of a portion of Ice Stream E of the Siple Coast area, West Antarctica (Fig. 1).

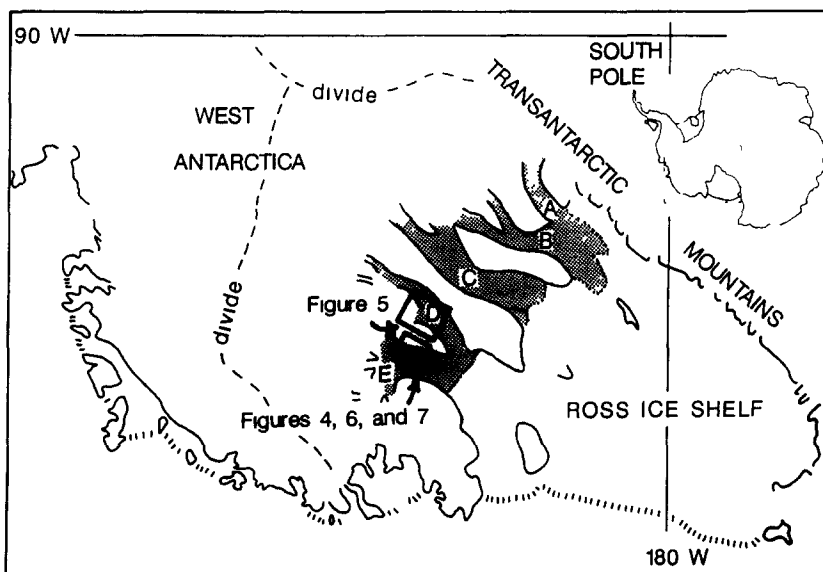


Figure 1 Location of the test areas used in this study. Labels refer to figures within text.

THE ALGORITHM

The image-to-image correlation algorithm we use is based on the normalized cross-covariance method (see Bernstein, 1983). The most common use of this type of algorithm in image processing is to locate accurately tie-point pairs in two images to coregister them. However, if an independent method for coregistration can be found, the algorithm may be used to find the displacements of moving features, provided that the features show little change in their appearance. Two software packages incorporating this algorithm were used in our analysis of ice velocities: Land Analysis System (LAS), developed by NASA (used by TAS and RAB), and SAMSON, developed by MacDonald Dettwiler and Associates (used by MJD and JCW).

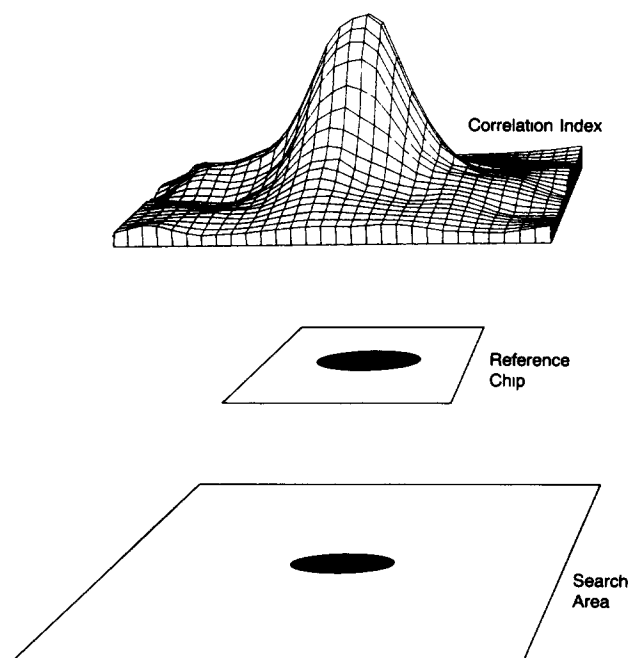
In the algorithm, for each small image chip selected from a reference image, a matching chip is searched for in a larger search area within a second image. The normalized cross-covariance correlation adjusts the intensity values of the two chips so that they have zero mean and unity standard deviation before correlating. This helps to deal with differences in illumination between the images, and produces a normalized result (in the range -1 to 1) so that the correlation results from various attempts within one search chip may be compared. The reference chip is compared to a chip of the search area at every center-pixel location in the search area for which the reference chip will fit entirely within the search area. The intensity values or digital numbers (DN), for pixels within chips are compared on a pixel-by-pixel basis. The similarity of the reference chip and the search area chips is quantified by the expression

$$CI_{(l,s)} = \frac{\sum_{l,s} (r_{(l,s)} - \mu_r)(s_{(l,s)} - \mu_s)}{\left[\sum_{l,s} (r_{(l,s)} - \mu_r)^2 \right]^{1/2} \left[\sum_{l,s} (s_{(l,s)} - \mu_s)^2 \right]^{1/2}},$$

where $CI_{(l,s)}$ is the correlation index between the two chips at the search-area chip center-pixel location L,S , $r_{(l,s)}$ is the DN for the reference chip pixel at location l,s , μ_r is the average DN for the reference chip, $s_{(l,s)}$ is the DN for the search-area chip pixel at location l,s , and μ_s is the average DN for the search-area chip. The expression has a maximum value of 1 when the reference chip and

search-area chip centered on pixel L,S have identical grey-scale values at each corresponding pixel location. A "map" of the correlation index is made from all the $CI_{(l,s)}$ values over the entire search area (see Fig. 2). From this map, a variety of correlation statistics are computed to evaluate the match, such as the maximum CI value, number of secondary peaks, mean and variance of the correlation surface, peak-above-mean, peak-above-second-peak, and full width at half maximum for the main peak. The two software packages differ somewhat in this evaluation; in LAS, a region around the maximum $CI_{(l,s)}$ value, the "peak region," is culled from the map prior to evaluating parameters such as peak-above-mean and standard deviation of the "background" correlation index, while SAMSON includes the peak area in its evaluation and calculates a greater variety of statistical parameters. SAMSON also allows more flexibility in applying the parameters as selection criteria for matches. A variety of combinations of peak-above-mean and peak-above-second-peak values were used in our studies to quality-control the matches. Good results for our study were obtained by limiting selected matches to cases where peak-above-mean was greater than 10 and

Figure 2 Schematic diagram of the cross-correlation algorithm. See text for description.



peak-above-second-peak was greater than 3, however, the success criteria may be somewhat case-specific. If the maximum $CI_{(L,S)}$ passes these tests, a biquadratic function is fit to the CI values in the peak region. The location of the maximum of this function (to ± 0.1 pixel accuracy) is the reported match location.

An important additional feature of the SAMSON software is the ability to automatically perform a reverse correlation for every feature matched. The reverse correlation takes the location of the maximum CI in the search area (the integer pixel location) and generates a reference chip around it. A search area centered on the location of the original reference chip (from the "forward" correlation) is examined for a match. The reverse correlation should result in a selected match point within one pixel location from the initial ("forward" correlation) reference chip center. If it does not, then the match is rejected. The essential idea behind reverse correlation is that the shift determined should be independent of which image is chosen as the reference image. A high proportion of false correlations can be detected by this method because only reasonable matches are likely to produce identical results for correlation in both directions.

IMAGE ACQUISITION AND PREPROCESSING

To maximize the similarity of the surface features in sequential satellite imagery, sun angle and azimuth should be nearly the same in both images, and differences between viewpoints for the two images should be minimized. This is best accomplished by acquiring scenes with the same scene center location (i.e., identical path/row locations for Landsat) taken at the same time of year. The time interval between the scene acquisition dates should be such that the slowest features to be measured have moved a distance equal to at least a few pixels on the images (based on an initial guess of their velocity). Precision of the derived velocity measurement increases with a greater time interval, however, an increased time interval raises the chance that the surface features have changed in appearance. For our study, two Landsat images of Path 7, Row 119 were used (ID#510511451 and ID#423411053). Acquisition

dates are 16 January 1987 and 12 December 1988. This temporal separation of nearly 2 years, coupled with the 28.5-m ground resolution of TM data, allowed us to measure ice speeds as low as 30 m/yr with a precision of ± 3 m/yr (Bindschadler and Scambos, 1991).

Four processing steps are used to enhance small ice surface features and remove noise prior to extracting displacement measurements: principal components transformation, scan-line destriping, high-pass filtering, and gaussian contrast stretching. The presence of clouds in either of the scenes may require additional, case-specific, steps in preprocessing. It is best if subscenes are chosen so that no clouds are present. In multiband image data the first principal component (PC1) of the visible and near-infrared data yields low-noise images in which ice topography is enhanced, and subtle reflectance differences between snow and firn, seen in some individual bands, are suppressed ("firn" is old, partially recrystallized, granular snow, see Orheim and Lucchitta, 1987, 1988). For this study, the PC1 of TM Bands 2, 3, 4, and 5 was used (Fig. 3b). Panchromatic digital image data, such as SPOT Panchromatic, could be used directly. Scan-line noise striping or banding (which remains in the PC1 image because it is correlated in all bands) is then removed (Fig. 3c). For TM data, several effective destriping algorithms are reported in Crippen (1989). High-pass spatial filtering is then applied to the images to remove brightness variations associated with large-scale topographic features, or ice "undulations" (Fig. 3d). Long-wavelength topographic undulations at the ice surface are due to the response of ice flowing over long-wavelength features in the underlying bedrock (Paterson, 1981). These features remain fixed while the small-scale surface features move with the ice. The use of these features for image coregistration is discussed later. For the measurement of small feature displacements, long-wavelength topography must be suppressed, or the brightness variations of the surface around a small feature will bias the cross-correlation algorithm, due to changes in sun aspect angle as ice flows over an undulation. The scale of the filter should be roughly equal to the thickness of the ice (Budd and Carter, 1971, see also discussion below). For the TM images used here, a 35×35 pixel kernel was used (equivalent to a ~ 1 km spatial filter window). The high-pass filtered PC1

image is then stretched to a gaussian distribution of brightness levels

ICE VELOCITY MEASUREMENT

Displacement measurements of features on the processed images may be made in two ways either by creating reference chips around visually selected features (as in Bindschadler and Scambos, 1991) or by generating a grid of equally spaced reference chips (as in the present study, see below) If some initial estimate of ice velocity is available, smaller search areas can be specified, which greatly reduces the computing time required

Unsuccessful matching situations are usually caused by one of three factors an absence of surface features, reflectance variations associated with the distribution of fresh snow and firn, or significant velocity gradients at the scale of the reference chips Boundaries between fresh snow and firn are transient features, changing after each storm, thus each image has its own pattern of new snow patches draped over the topography of the area Although principal components processing suppresses the reflectance variations associated with snow/firn boundaries, they are still present The boundaries are sharp features, and thus are not removed by high-pass spatial filtering In high-velocity-gradient areas, such as at the margins of an ice stream or glacier, shear distortion of the surface features and changes in the relative positions of features can occur at the scale of the reference chip In general, velocity gradients are gradual enough that with reasonably sized image chips and net ice motions of a few to a few tens of pixels, distortions are too small to hamper the matching algorithm However, the difficulties associated with high-shear areas can be addressed by changing the size or shape of the reference chip Smaller chips, or chips that are elongated parallel to the direction of flow, will have less distortion (Note SAMSON allows only square image chips, LAS allows for rectangular chip sizes, but with limits on the size ranges)

A comparison of ice speeds measured by both the cross-correlation technique discussed here and the manually-based point-picking method used in previous studies is shown in Figure 4 The test area is a central portion of the upstream

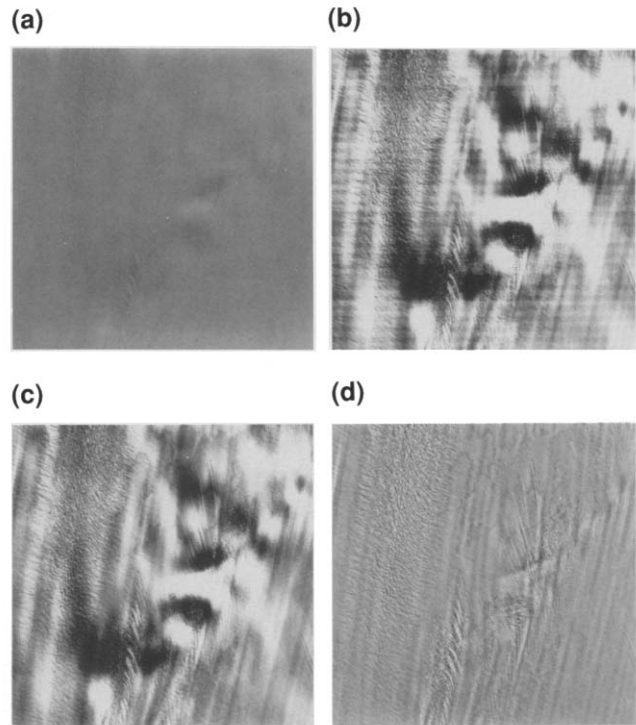


Figure 3 Landsat TM images of the central portion of Ice Stream E illustrating the four preprocessing steps used to enhance the images prior to measuring the displacement of small surface features Image a is a raw TM Band 4 image of the area Image b is a first principal component image (PC1) using Bands 2, 3, 4, and 5, this image has been stretched to reveal the scan-line striping in the data Image c is a PC1 image after a destriping algorithm has been applied Image d is a high-pass filtered image derived from c, using a 35×35 pixel kernel In practice, the image data is not stretched until after the high-pass filtering step Flow direction is from top to bottom, parallel to flow bands Sun direction is to the upper right

area of Ice Stream D (unpublished data) For each point, both methods were used, the pointlike features selected and measured manually were used as chip center-points for the cross-correlation program The small y -intercept, near-unitary slope, and high R^2 value (0.964) of the Figure 4 data indicates that the cross-correlation method imparts no systematic error to the displacements and is generally consistent with velocities determined by visual methods At present, there is no "ground truth" on ice-stream velocities in the imaged area

COREGISTRATION OF IMAGES

As noted above, long-wavelength features in the ice surface ("undulations") remain fixed relative

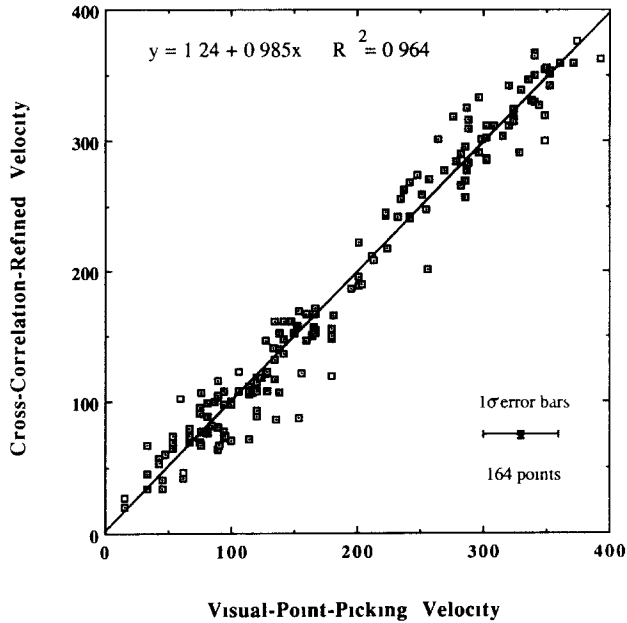


Figure 4 Comparison of the cross-correlation-refined speeds with visual-point-picking techniques similar to those used in previous studies. Data are from Ice Stream D (unpublished data). Speeds are in m/year.

to the smaller-scale features which move with the ice. This permanence permits their use in coregistration of the images. Long-wavelength undulations in ice-sheet topography are visible in enhanced satellite imagery in many areas (e.g., Dowdeswell and McIntyre, 1987, Lucchitta et al., 1989, Swithinbank, 1988), particularly in areas of moving ice (Bindschadler and Vornberger, 1990, Stephenson and Bindschadler, 1990). In a study of the relationship of the surface topography of

moving ice and the underlying bedrock features, Budd and Carter (1971) determined that undulations are directly correlated with bedrock topography, specifically, with the first derivative of the bedrock surface. Response of the ice surface is greatest to bedrock features with wavelengths of about 3.3 times the ice thickness. Response of the surface falls off rapidly below wavelengths less than one ice thickness. Thus, an image of ice surface topography at wavelengths greater than about one ice thickness is dominated by features related to bedrock topography.

Despite their diffuse outlines, these features can provide accurate coregistration of images using the cross-correlation algorithm, if a sufficiently large reference chip and search area are used. The reference chip must be large enough to encompass several undulations. In this application, low-pass spatial filtering of the destriped PCI images is required to remove the small-wavelength features (Fig. 5). Because of the large reference and search areas involved, the technique is very computer-intensive. Computation time may be reduced by estimating the best fit of the undulation field prior to a run, and selecting a search area only slightly larger than the reference chip. This may be accomplished by visually matching the undulation fields, that is, rapidly alternating or "flickering" between the two undulation fields and adjusting the relative positions until the fields match up. This visual matching of the undulation fields can result in a coregistration accuracy of about ± 1 pixel (see Bindschadler and Scambos, 1991).

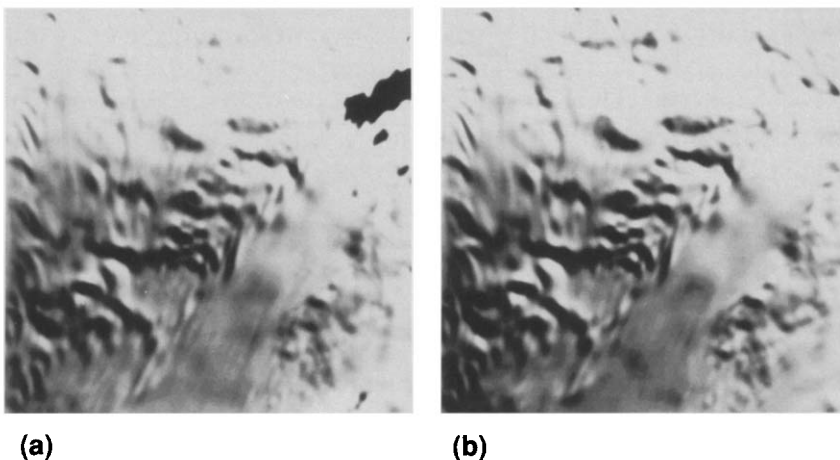


Figure 5 Low-pass-filtered PCI images of the central portion of Ice Stream D, showing the undulation fields used for coregistering the images. The dark area in the upper right corner of the left image is cloud shadow. The left image was taken 16 January 1987, the right image was taken 12 December 1988. Sun direction in both images is towards upper right. The filter kernel used was 35×35 pixels, or nearly $1 \text{ km} \times 1 \text{ km}$.

A test of the computer-based coregistration technique, using the cross-correlation algorithm, matched the undulation field in the central portion of Ice Stream D to an accuracy of ± 0.8 pixels. To generate the undulation image, low-pass filtering with a 35×35 pixel filter kernel was used on the destriped PC1 image (based on a rough estimate of 1 km ice thickness). For this test, LAS software was used. Subsampling of the images is required for LAS software, because the maximum size of the reference image chip is limited to 128×128 pixels. This chip size does not encompass enough of the undulation field at full resolution to accurately coregister the images. Therefore, the low-pass-filtered undulation field images were "shrunk" to 30% of their original size. A grid of 36 reference chips of 128×128 pixels was used on 750×750 pixel images (subsampling from 2500×2500 pixel images derived from the same Landsat scenes mentioned earlier). Search areas were 16 pixels larger than the reference chips in both line and sample directions, and were placed close to the expected match (a coregistration vector of +22 lines and +156 pixels) determined by the visual flickering technique. Thirty-one successful correlation matches were found, yielding an average registration vector of $+21.9 \pm 0.2$ lines and $+156.1 \pm 0.3$ samples. Error magnification due to subsampling yields the quoted accuracy of just under ± 1 pixel. The SAMSON software does not have a limitation on image chip size, thus, although coregistration using SAMSON with larger chip sizes would be even more computer-intensive, the result should yield a more accurate coregistration than with LAS.

HIGH-RESOLUTION VELOCITY MAP OF THE CENTRAL AREA OF ICE STREAM E

As a demonstration of the potential of the velocity-measuring technique, a high-resolution map of the velocity field of the central portion of Ice Stream E is presented in Figure 6. The map is based on 311 displacement measurements using the cross-correlation method. Three grids of reference chips were generated, with chip sizes of 32×32 , 64×64 , and 128×128 pixels. Search areas were 32 pixels larger than the reference chips in both line and sample directions, and centered on grids of locations using an initial-guess velocity of 350

m/a downstream (based on the results reported in Bindshadler and Scambos, 1991). Three chip sizes increased the chances of successful correlations in both high-velocity-gradient areas and areas of subtle surface features. The results of the 128×128 pixel reference-chip grid runs were used only where smaller grid sizes failed to find a suitable match. In 855 attempted displacement measurements, the algorithm found a correlation in 413 cases. Of these, 75 of the 128×128 pixel reference-chip matches were eliminated from areas that were mapped in greater detail by smaller chip sizes. Twenty-seven matches using other chip sizes were eliminated as being inconsistent with surrounding data or ice features. The points were not reverse-correlated because the displacements were measured using LAS software. The areas in the image where the algorithm failed to find matches were characterized by nearly featureless snow surface or by the presence of snow-firn boundaries in one of the images. In the chosen test area, velocity gradients were not large enough to cause the distortion problems noted in earlier studies (Bindshadler and Scambos, 1991), given the chip sizes and time interval used.

The velocity maps in Figures 6a and b show the detail revealed by high-resolution mapping and the consistency of the measured velocity field. This area of Ice Stream E was selected because earlier mapping (Bindshadler and Scambos, 1991, see Fig. 7) suggested that a local minimum was present and that high velocity gradients surrounded it, possibly correlated with shear crevassing observed in the image. Figure 6 confirms this pattern, and provides a more robust characterization of it. High-velocity-gradient areas to the left of the velocity minimum are associated with the onset of crevassing, with crevasse orientation suggesting a left-lateral shear. Extensional crevassing downstream from the velocity minimum also correlates with a positive velocity gradient. Figure 6b demonstrates the sensitivity of the algorithm to changes in flow direction. Ice-flow direction changes of a few degrees, in response to the "ridge" of topographic features on the right side of the image, are well defined by the velocity field. The ability to determine flow direction accurately enhances the glaciological uses of these data. This accuracy is a result of the subpixel interpolation of displacements used by the correlation algorithm.

(a) **Speed, meters/year**



(b) **Flow Direction**
(degrees, relative to edge of ice stream)



Figure 6 Speed and flow direction contours superimposed on an image of a central portion of Ice Stream E. Points where successful correlations were made are shown as white dots on the image. Flow direction is from top to bottom, parallel to the flow bands in the image. The flow angles contoured in Figure 6b are referenced to the stream edge, located off the image to the right, with a near-vertical upper-right-to-lower-left orientation, see Figure 7. Positive values represent flow vectors clockwise of this orientation, and negative values represent flow vectors counter-clockwise of it.

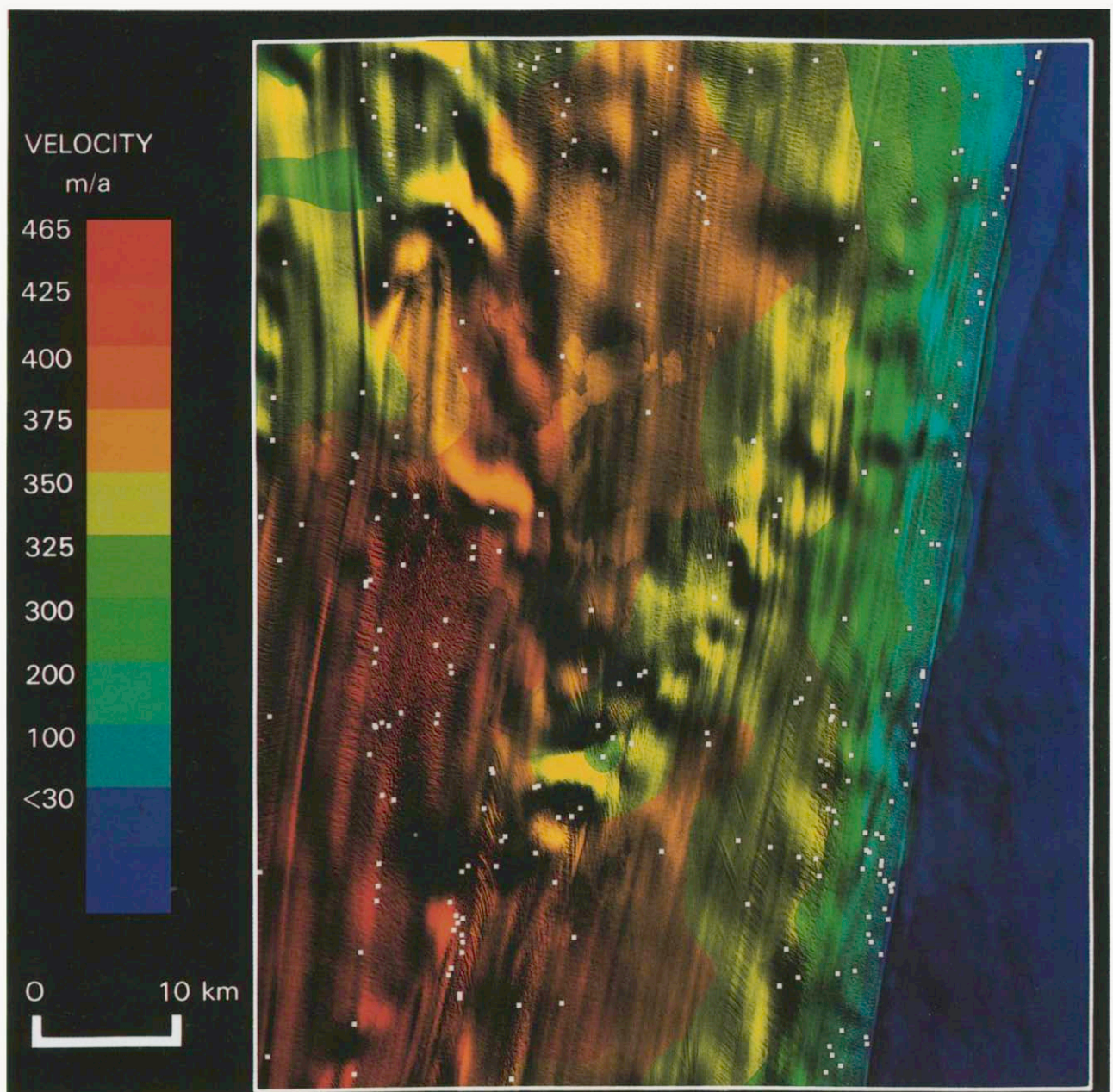


Figure 7 Hue-intensity-saturation image of Ice Stream E and its velocity field. The image was generated using the first principal component of TM Bands 2, 3, 4, and 5 as intensity, and ice velocity [as reported in Bindschadler and Scambos (1991)] as hue. Saturation is constant. The color velocity scale is nonlinear to emphasize velocity variations within the main body of the ice stream.

Figure 7 illustrates another way of integrating velocity field data with Landsat imagery of an ice stream by using an intensity-hue-saturation transform. The image shows the velocity field and surface features of a larger portion of Ice Stream E (data from Bindschadler and Scambos, 1991). In the image, ice speed determines the hue, while topography, as represented by an unfiltered PC1

image, determines the intensity. Saturation is constant. White dots in the image are locations of velocity measurements. This type of processing, coupled with the accurate velocity mapping provided by the presented technique, helps illustrate the close connection between variations in the velocity field and the formation of surface features on the ice.

FUTURE WORK AND ADDITIONAL APPLICATIONS

Application of the above-described methods to other areas of these ice streams (currently underway) will provide a regional velocity map of the area. The high density and accuracy of the velocity data provided by the technique makes it possible to extract meaningful strain-rate information as well, again on a regional scale. Several other outlet glaciers in Antarctica and Greenland, such as Pine Island or Byrd Glaciers, are potentially good areas to apply the described methods, since duplicate satellite imagery already exists and initial velocity measurements using the point-picking method have already been made (MacDonald et al., 1989). Further, the velocity fields of ice shelves, as well as those of ice sheets, may be characterized by this method, if coastlines or ice rises provide an adequate basis for coregistration, and if a sufficient number of surface features are revealed by image enhancement (e.g., Doake and Vaughan, 1991).

The statistical robustness of the cross-correlation method represents a great improvement over previous methods for displacement measurements from sequential imagery. Although the demonstration of the algorithm has concentrated on the glaciological aspect of measuring ice-stream motion, there is a wide range of possible applications in other areas of environmental research. The only requirements are that the image data be digital, that the moving features show little change between images, and that some means exists for coregistering the images.

This work was supported by an NSF/DPP-8614407 grant. The authors wish to thank Nisha Gulra for her assistance in evaluating the algorithm, and Dr Robert Massom for helpful comments on early drafts of the manuscript. The comments of the reviewers improved the work, and are greatly appreciated.

REFERENCES

- Bernstem, R. (1983), Image geometry and rectification, in *Manual of Remote Sensing* (R. N. Colwell, Ed.), American Society of Photogrammetry, Falls Church, VA, pp. 881–884.
- Bindschadler, R. A., and Scambos, T. A. (1991), Satellite-image-derived velocity field of an Antarctic ice stream, *Science* 252 242–246.
- Bindschadler, R. A., and Vornberger, P. L. (1990), AVHRR imagery reveals Antarctic ice dynamics, *Eos* 71 741–742.
- Budd, W. F., and Carter, D. B. (1971), An analysis of the relationship between the surface and bedrock profiles of ice caps, *J. Glaciol.* 10 197–209.
- Crippen, R. E. (1989), A simple filtering routine for the cosmetic removal of scan-line noise from Landsat TM P-tape imagery, *Photogramm. Eng. Remote Sens.* 55 327–331.
- Doake, C. S. M., and Vaughan, D. G. (1991), Rapid disintegration of the Wordie Ice Shelf in response to atmospheric warming, *Nature* 350 328–330.
- Dowdeswell, J. A., and McIntyre, N. F. (1987), The surface topography of large ice masses from Landsat imagery, *J. Glaciol.* 33 16–23.
- Lucchitta, B. K., and Ferguson, H. M. (1986), Antarctica measuring glacier velocity from satellite images, *Science* 234 1105–1108.
- Lucchitta, B. K., Ferguson, H. M., Schafer, F. J., Ferrigno, J. G., and Williams, R. S., Jr. (1989), Antarctic glacier velocities from Landsat images, *Antarctic J. U. S.* 24 106–107.
- MacDonald, T. R., Ferrigno, J. G., Williams, R. S., Jr., and Lucchitta, B. K. (1989), Velocities of antarctic outlet glaciers determined from sequential Landsat images, *Antarctic J. U. S.* 24 105–106.
- Orheim, O., and Lucchitta, B. K. (1987), Snow and ice studies by Thematic Mapper and Multispectral Scanner Landsat images, *Ann. Glaciol.* 9 109–118.
- Orheim, O., and Lucchitta, B. K. (1988), Numerical analysis of Landsat Thematic Mapper images of Antarctica: surface temperatures and physical properties, *Ann. Glaciol.* 11 109–120.
- Paterson, W. S. B. (1981), *The Physics of Glaciers*, Pergamon, Oxford, pp. 164–167.
- Stephenson, S. N., and Bindschadler, R. A. (1990), Ice-stream evolution revealed by satellite imagery?, *Ann. Glaciol.* 14 273–277.
- Swifthbank, C. (1988), Antarctica, U. S. Geological Survey Professional Paper 1386-B, U. S. Government Printing Office, Washington, DC, 278 pp.